JOURNAL OF PROPULSION AND POWER
Vol. 14, No. 5, September–October 1998

Effects of Periodic Atomization on Combustion Instability in Liquid-Fueled Propulsion Systems

W. E. Anderson,* K. L. Miller,† H. M. Ryan,‡ S. Pal,§ and R. J. Santoro¶
Pennsylvania State University, University Park, Pennsylvania 16802
and
J. L. Dressler**
Fluid Jet Associates, Spring Valley, Ohio 45370

A detailed understanding of the mechanism by which combustion instability occurs in liquid rocket engines does not exist. This paper examines the specific role that atomization may play in combustion instability. The effects of mean drop size, drop size distribution, and atomization periodicity are examined explicitly with a combustion response model, whose results indicate that all of these effects are important. It is shown that periodic atomization results in large variations in the magnitude of the pressure response when the atomization frequency is within a factor of 10 of the acoustic oscillation frequency. These results are consistent with an explanation of an empirical stability correlation, whereby the nonuniform and unsteady production of drops is a controlling factor in the growth of combustion instabilities. Experimental results from a subscale rocket combustor that support the importance of periodic atomization are presented. Atomization was electromechanically forced at frequencies from 2000 to 8000 Hz to accentuate the natural tendency for periodic atomization associated with impinging jet injectors. High-amplitude pressure oscillations at frequencies corresponding to the forced atomization frequencies substantiate the importance of periodic atomization. Pressure oscillation amplitudes approaching 10% of mean chamber pressure were measured when the drivers were operating at near optimal conditions. A conceptual model that is consistent with both these results and the empirical correlation is provided.

Nomenclature

a = sound speed
d = diameter
f = frequency or number distribution
h = sheet thickness
m = mass
m' = unsteady vaporization rate
$\dot{m}$ = mass flow rate
p' = unsteady pressure amplitude
R = response factor
S = ρ_{amb}/ρ_j
t = time
U = velocity
v = velocity
We = Weber number
x = axial distance from impingement point
α = spray angle
γ = specific heat capacity ratio, c_p/c_v
θ = impingement half angle
λ = wavelength
ρ = density
σ = surface tension
ϕ = phase angle or angular coordinate on the sheet
ω = radial frequency

Subscripts
amb = ambient
atom = atomization
b = breakup
beat = beat
CL = centerline
coolant = coolant
d = drop
f = fuel
g = gas
inst = instability
j = jet
l = liquid
lig = ligament
o = initial or orifice
oxidizer = oxidizer
trans = transverse
1 = jet 1
2 = jet 2
10 = arithmetic mean
32 = Sauter mean

Received Sept. 2, 1997; revision received March 31, 1998; accepted for publication May 4, 1998.

*Research Associate, Department of Mechanical Engineering; currently Senior Principal Propulsion Engineer, Orbital Sciences Corporation, Chandler, AZ 85248. E-mail: andersonw@orbital-lsg.com. Member AIAA.
†Research Assistant, Department of Mechanical Engineering. E-mail: K1M156@psu.edu.
‡Research Assistant, Department of Mechanical Engineering; currently Development Associate, Praxair, Inc., Tarrytown, NY 10591. E-mail: harry_ryan@praxair.com.
§Senior Research Associate, Department of Mechanical Engineering. E-mail: s9p@email.psu.edu. Member AIAA.
¶Professor, Department of Mechanical Engineering. E-mail: rjs@email.psu.edu. Member AIAA.
**President/Owner. E-mail: dressler@erinet.com.

Introduction

FOR many launch applications the use of liquid (noncryogenic) fuel is desirable. Liquid fuels, i.e., hydrocarbons (HC), are much denser than hydrogen and easier to handle. These attributes are particularly advantageous for the first stage of a multiple-stage, low-cost system, for instance, or for launch-on-demand applications. Usually, liquid oxygen (LOX) is used in conjunction with liquid HC fuels. A major issue in

the development of LOX/HC rocket engines is whether the occurrence of combustion-generated pressure oscillations, which could lead to catastrophic failure, can be avoided.

The initiation and growth of these pressure oscillations, commonly referred to as "combustion instabilities," are primarily determined by the design of the injector. A good injector design provides oscillation-free operation and acceptable thrust efficiency throughout the operating envelope. Historically, LOX/HC rocket engines have had thrust efficiencies of 3–5% less than their hydrogen-fueled counterparts.[1] This is not because design strategies for efficient combustors are unknown, but rather because the design strategies that lead to very efficient combustion also tend to promote the occurrence of high-frequency combustion instability in LOX/HC rocket engines.

Instabilities can be classified according to whether they occur as bulk mode oscillations or in resonance with the chamber's acoustic modes, as well as by the mechanisms by which they are initiated and amplified.[2,3] Pressure oscillations that are due to fluctuations in the propellant flow rate are referred to as injection-coupled instabilities. Injection-coupled instabilities are amplified when the flow rate oscillations become coupled with either bulk- or acoustic-mode chamber pressure oscillations. Eliminating injection-coupled instabilities (chug instabilities) is accomplished by increasing the injection pressure drop (by reducing the injection flow area, or by increasing the propellant flow rate). Acoustic mode instabilities, which occur at a higher frequency than chug instabilities, can also be because of injection coupling. Longitudinal-mode instabilities are often injection coupled and are acoustic in nature with a pressure antinode at the injector face. Injection-coupled instabilities are well modeled with conventional time lag models and are relatively easy to avoid or eliminate.

More problematic than the injection-coupled instabilities are the instabilities that are intrinsically coupled to the combustion processes. These intrinsic instabilities typically occur with liquid propellants when the energy release density in the combustor is increased; as the energy release density increases, higher modes of combustion instability occur. To eliminate these instabilities, the injection pressure drop is reduced or the injector element orifice size is enlarged, both of which tend to decrease energy release density and combustion efficiency in a fixed volume combustor. This purposeful decrement of performance to achieve combustion stability is the reason that LOX/HC rocket engines such as the H-1 and F-1 have lower combustion efficiencies than do hydrogen-fueled rocket engines.

To develop effective design strategies for the elimination or control of combustion instabilities, it is necessary to define the physical mechanisms that lead to the growth of these instabilities. Most of the work to date on combustion instability mechanisms has been based on the premise that intrinsic instabilities are controlled by vaporization. This premise is based explicitly on the proposition that vaporization is the rate-limiting step in spray combustion. The role of atomization has been dismissed largely on the basis that atomization occurs so rapidly that it could not be rate controlling.

Previous work conducted in our laboratory emphasized measurements of a cold-flow spray formed by impinging jet injectors, which are commonly used with liquid propellants.[4] The measurements included atomization frequency and drop size distribution. The experimental results were compared with an empirical stability correlation for the highest sustainable frequency of combustion instability in rocket engines that use impinging jet injectors.[5,6] It was found that atomization is a periodic phenomenon that occurs on a time scale similar to typical combustion instabilities. Furthermore, the atomization frequency and the highest sustainable frequency of combustion instability indicated by the empirical stability correlation increase linearly with the ratio of injection velocity-to-orifice diameter (U_j/d_o). The measurements also indicated that the average drop size and the polydispersity of the drop size distribution decreased with increasing U_j/d_o.

Although the impinging jet measurements indicated a clear periodic nature to the atomization process, there was a definite unsteady character evident as well.[5,6] Even though an average frequency was determined that was three to four times higher than the highest sustainable frequency indicated by the empirical correlation, some variation in the atomization frequency occurred. It is argued that under such conditions, interactions with the acoustic field of the combustion chamber will determine which frequency, if any, will intrinsically couple to the combustion process.

To investigate this topic further, the present work considers both theoretical and experimental approaches to gain further insights. In the theoretical approach a model is developed that allows the combustion response calculation that is a result of the vaporization process when periodic atomization is included. In the experimental approach a novel electromechanical modulation technique is used to affect the atomization frequency. This modulation results in a sharper periodic atomization frequency compared with the previously studied unsteady case. Although the modulation is applied to the liquid flow in the injector, it is argued that this approach preferentially establishes a narrow frequency range for the periodic atomization from among the broader atomization frequencies occurring naturally. Thus, this approach still allows the examination of intrinsic combustion instability behavior.

Analysis

Model Description

The combustion response methodology is a standard approach for analyzing combustion stability.[7] In this analysis the changes in the combustion rate because of ambient oscillations are calculated and integrated to determine the amount of the heat release that occurs in phase with the pressure oscillation. A large positive value of combustion response at a given frequency indicates that a potential for a coupling between acoustic oscillations and heat release exists if the frequency corresponds to an acoustic mode of the chamber; combustion instability may then occur.

Usually the combustion response is approximated by the vaporization response. The in-phase response factor R is defined as

$$R = \int_0^{t_d} m'p' \, \mathrm{d}t \Big/ \int_0^{t_d} (p')^2 \, \mathrm{d}t \tag{1}$$

where t_d is the drop lifetime. In the present implementation of the combustion response analysis, an open-loop response is calculated. Theoretically, a value of R of at least $(\gamma + 1)/2\gamma \sim 0.9$ is required to drive a longitudinal instability for the case of concentrated combustion at the pressure antinode of a closed chamber, where γ is the specific heat capacity ratio of the gas. In the present analysis, the Priem–Heidmann model is used to calculate the vaporization rate.[8]

A standing transverse acoustic wave in a two-dimensional chamber was considered in the analysis, thus, the pressure oscillates in a sinusoidal fashion:

$$p' \propto \cos(\omega t) \tag{2}$$

The pressure oscillations are accompanied by out-of-phase transverse velocity oscillations:

$$v_{\text{trans}} \propto \sin(\omega t) \tag{3}$$

The maximum amplitude of the pressure oscillation was set at 0.1 times the mean chamber pressure. The order of the amplitude of the transverse velocity oscillation associated with a

pressure oscillation of p' is $(a/\gamma)p'$. This condition corresponds to a location in the chamber that is intermediate between a pressure antinode and a pressure node, where both oscillations in velocity and pressure are present.

The combustion response analysis is a straightforward and mechanistic means of predicting combustion stability characteristics. Accurate accounting of the combustion processes is the main difficulty. Of all the component combustion processes, atomization is possibly the most difficult to model accurately. Consequently, most applications of the combustion response analysis greatly simplify the atomization process. Typically, an array of drops, all of the same size, is used to represent the actual distribution of drop sizes and velocities. The representative drop is injected continuously over one cycle of the pressure oscillation. These injection rates range from about 16 to 36 times per cycle.[7,9] However, the effects of periodic atomization and drop size distribution should be included in the analysis.

A phenomenological model of atomization for impinging jet injectors was developed earlier and will only be briefly reviewed here.[10] The phenomenological model has three main steps: 1) Fan formation and the appearance of impact waves, 2) fragmentation of the fan into ligaments and other large structures, and 3) the disintegration of ligaments and large drops into small drops that represent the quasiequilibrium end state of atomization. Impact waves are observed to form directly following the impingement of the liquid jets and have a characteristic length on the order of the jet diameter. These waves are convected down the sheet at a speed equal to the liquid jet velocity. Thus, the highest atomization frequency predicted by this model corresponds to $U/\lambda \sim U_j/d_o$, and is shown in Fig. 1 expressed in terms of a Strouhal number as $fd_o/U_j \sim 1$. This highest atomization frequency is compared to results from an empirical stability correlation of the highest sustainable frequency of combustion instability (referred to as the high-frequency cutoff) that can be driven by a given impinging jet injector design. It is seen that the highest sustainable frequency of combustion instability is about 10 times less than the highest atomization frequency. This will be shown to have a major impact on the magnitude of the combustion response. The fact that the atomization frequency and the highest sustainable frequency of combustion instability are both described by the same nondimensional parameter suggests a strong coupling mechanism between periodic atomization and combustion instability.

A model was developed that accounted for the processes described in the preceding text.[10] The average size of the ligaments, d_{lig}, that are shed off the leading edge of the liquid fan can be determined from the wavelength of the impact waves λ and the thickness h_b of the sheet at the point where the sheet breaks up as discussed in Ref. 10, i.e.,

$$d_{\text{lig}} = \sqrt{4\lambda h_b/\pi} \tag{4}$$

where h_b can be determined from[11]

$$h_b = \frac{d_o^2 \sin^3\theta}{4x_b(1 - \cos\phi\cos\theta)^2} = \frac{d_o^2}{4x_b} f(\theta) \tag{5}$$

A correlation for the dependence of λ on x_b from data obtained in cold flow studies[10] yields

$$\lambda/d_o = 0.687 + 0.1019(x_b/d_o) \tag{6}$$

Furthermore, because x_b also changes with ambient pressure, a correlation was developed for x_b as a function of jet conditions and ambient pressure based on the product of the square of the density ratio $s = \rho_{\text{amb}}/\rho_j$, and the jet Weber number We_j[10]

$$x_b/d_o = 13.56(We_j s^2)^{-0.102} \tag{7}$$

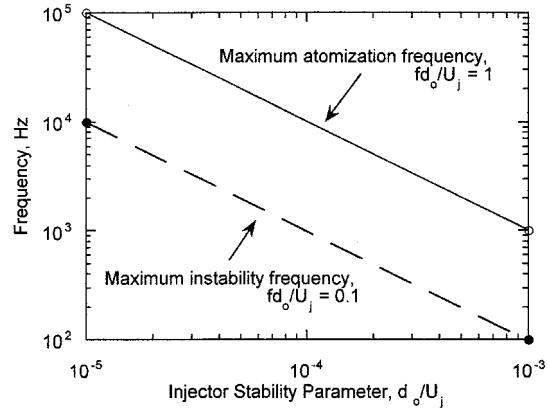

Fig. 1 Comparison of atomization frequencies associated with impinging jet injectors and combustion instability frequencies.

Equations (4–7) can be combined to yield an equation for the average diameter of a ligament shed off the liquid fan. Because most drop size measurements have been taken at the centerline of the fan, i.e., $\phi = 0$, the centerline ligament diameter was calculated to be

$$\left.\frac{d_{\text{lig}}}{d_o}\right|_{\text{CL}} \approx 0.22\sqrt{\left[\frac{f(\theta)}{\pi}\right][(We_j s^2)^{0.102} + 2]} \tag{8}$$

The disintegration of the ligaments into drops was also treated through a correlation for d_{32}/d_{lig} that relies on Eq. (8) and correlations that exist for drop size as a function of impinging jet geometry and flow conditions[12] (also see Ref. 10), and yields

$$\frac{d_{32}}{d_{\text{lig}}} = 1.008(We_{g,\text{lig}})^{-0.136} \tag{9}$$

where $We_{g,\text{lig}}$ is the ligament Weber number based on the gas density. Finally, using Eqs. (6) and (7) to determine the wavelength of the impact waves λ, and the fact that the impact waves travel along the sheet at a velocity U_j, the atomization frequency predicted by the model can be calculated (Table 1).

The combustion response analysis used here considers heptane drops burning in an oxygen environment. The measured size distribution for a water spray formed by impinging jets was converted to a heptane spray size distribution by accounting for the property differences of ambient gas density, liquid density, and surface tension by using the following correlation[12]:

$$d_d \propto \sigma^{0.16}(\rho_l/\rho_g)^{0.1} \tag{10}$$

The ambient pressure chosen for the study was 1.72 MPa (250 psia), which is approximately the nominal design pressure of the combusting flow tests that proceeded in parallel. The molecular weight of the products of heptane–oxygen combustion is 30 kg/kmole and the ambient gas temperature was chosen to be 3500 K. The resultant heptane drop size distribution used in the combustion response analysis is shown in Fig. 2. Note that the distribution was based on the measured water spray and adjusted for property differences. Table 1 provides a summary of the cases considered in the combustion response analysis at the conditions employed in the analysis, including the stability parameter d_o/U_j, the high-frequency cutoff based on the empirical stability correlation,[5] and the atomization frequency as calculated from an atomization model developed earlier.

Results

The vaporization rates of the drops under nonoscillatory conditions are shown in Fig. 3. The rates are normalized by

Table 1 Study cases used in response analysis of heptane/oxygen combustion

Case number	d_o/U_j, seconds $\times 10^{-5}$	High-frequency cutoff, Hz	Atomization frequency, Hz	d_{10}, μm	d_{32}, μm
1	2.59	3861	15,914	110	372
2	3.43	2915	11,529	133	389
3	4.10	2439	9,391	154	455
4	5.12	1953	7,272	182	472
5	9.98	1002	3,365	383	576

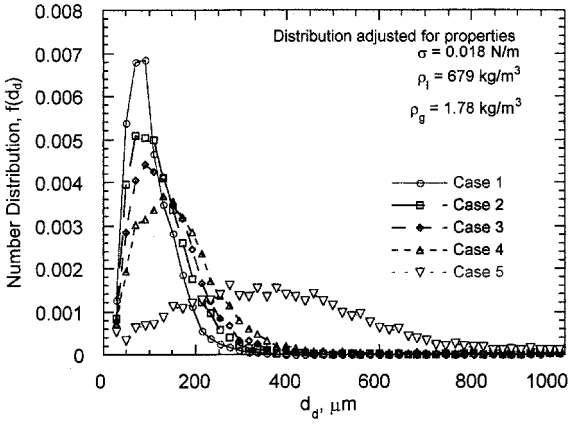

Fig. 2 Number distribution of heptane drops used in the combustion response analysis.

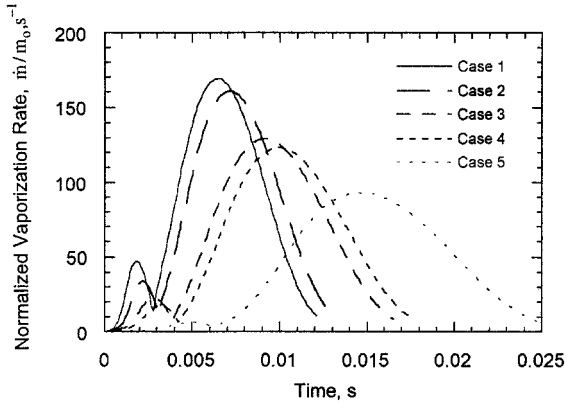

Fig. 3 Normalized vaporization rate of a heptane drop.

the initial mass of the drop m_o. The smallest mean-size drop (case 1, $d_{32} \sim 372$ μm) vaporizes within 12 ms, whereas the largest drop (case 5, $d_{32} \sim 576$ μm) takes about 25 ms to vaporize. The drop undergoes a regime where the difference between its velocity and the ambient gas velocity is a minimum, and this regime is indicated most clearly by the local minima in the vaporization rate. This regime, which occurs at about 3 ms for the smallest drop (case 1) and at about 6 ms for the largest drop (case 5), is the regime that Priem and Guentert regarded as being most unstable because here the drops are most susceptible to transverse velocity oscillations associated with the unsteady flowfield.[13]

Three different approaches were used to calculate vaporization response. The first approach is conventional and uses a mean drop size (d_{32}) to represent the spray. The continuous atomization approximation is used. For the second approach, the distribution of heptane drops shown in Fig. 2 is injected continuously over the period of oscillation. For both approaches using continuous atomization, the time interval between each injection was 1/16 of the period of oscillation, which is the value recommended in the ROCCID code.[14] Each of these approaches also uses the experimental data from Table 1 and Fig. 2 as input to the model. Because the drop size is dependent on the atomization frequency, it is difficult to uncouple the effects of drop size and atomization frequency. Thus, the third approach is a parametric study of the effects of periodic atomization on the combustion response of a single drop of a given size when the atomization frequency is on the same order as the pressure oscillation frequency.

Mean Drop Size, Continuous Atomization

Figure 4 shows the vaporization response of continuously atomized drops with a diameter equal to the Sauter mean diameter (d_{32}) of the distribution. The frequency at which the peak response occurs is inversely proportional to drop size, and ranges from about 60 Hz for the 576-μm drop to about 110 Hz for the 372-μm drop. The magnitude of the peak response is essentially independent of drop mean diameter and is about 0.75. These results are consistent with many of the response calculations reported previously that indicated response magnitudes too low to drive an instability.[7,9,15] The frequencies corresponding to the predicted peak response magnitude, which are dependent on the drop mean diameter, are much lower than the high-frequency cutoff values indicated in Table 1.

Size Distribution, Continuous Atomization

Figure 5 shows the vaporization response for the continuously atomized distribution of drops. The peak vaporization responses are attenuated by about 50% as compared to those of the continuously atomized mean drop sizes. For case 1, the case with the smallest mean drop size and the least disperse distribution, the peak response is 0.32 and occurs at a frequency of about 900 Hz. The peak response magnitude for case 5, having the largest mean drop size and the most disperse distribution, is 0.31 at a frequency of about 100 Hz. The magnitude of the response is insufficient to drive an instability for either the mean drop size-based or the distribution-based method. The use of the drop size distribution rather than the mean drop size also has an effect on the width of the response.

A comparison of the peak response frequencies predicted by the combustion response model with the high-frequency cutoff predicted by the empirical stability correlation (see Table 1) reveals that either application of the response analysis tends to underpredict the most amplified frequency. It is important to note that the empirical stability correlation does not necessarily represent the frequency with the highest growth rate; rather, it is the highest frequency of instability that has been observed in practical combustors.

Effects of Unsteady Atomization

Calculations were also done where the atomization frequency listed in Table 1 was used in conjunction with the drop size distribution of Fig. 2. This is a more realistic case than was considered in either of the prior two approaches. The calculated combustion response magnitudes for this periodic atomization case were significantly larger than for the case of drop size distribution with continuous atomization. The combustion response magnitude was also dependent on the phase angle ϕ between the pressure oscillation and the onset of periodic atomization. A parametric study of the effects of periodic atomization was performed because the exact relationship between atomization and the pressure oscillations can only be assumed. Drops with diameters ranging from 10 to 100 μm and atomization frequencies ranging from 5 to 15 kHz were

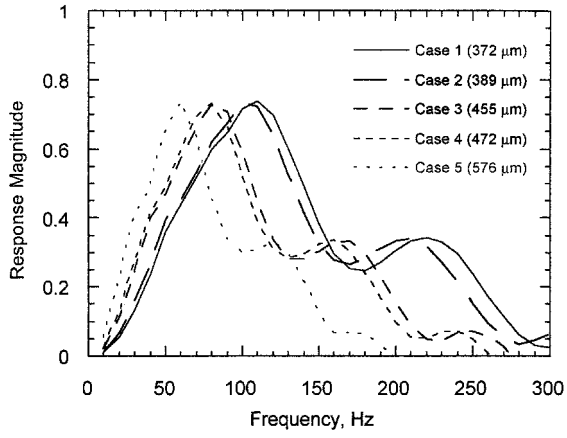

Fig. 4 Vaporization response magnitude for continuously atomized, mean-sized heptane drops as a function of ambient pressure oscillation frequency.

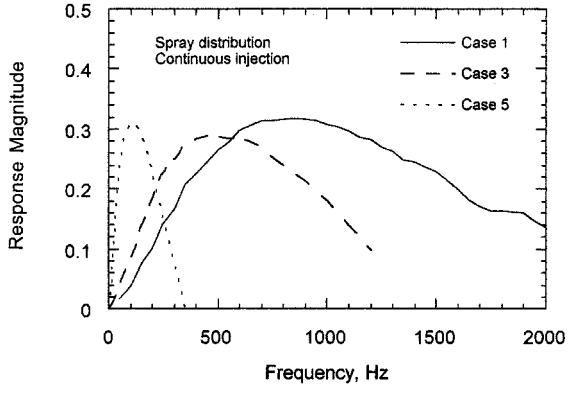

Fig. 5 Vaporization response magnitude for continuously atomized heptane drops with a drop size distribution shown in Fig. 2 as a function of ambient pressure oscillation frequency.

varied independently to evaluate their effects on the response function.

Representative results of the calculated response magnitude as a function of ambient pressure oscillation frequency and phase angle are shown in Fig. 6 for the 50-μm drop size case. For this case, the atomization frequency was 10 kHz. For all cases with periodic atomization, the peak response factor was significantly greater than 1, even approaching a value of eight for the 10-μm drop size case (not shown). Calculations indicated that the peak response magnitude decreased with increasing drop size. With increasing drop size, the peak response frequency was also reduced. These results indicate the potentially dominating effects of periodic atomization on response magnitude and, thus, the growth of the instability.

The effects of periodic atomization and drop size on the calculated peak response magnitude are shown in Fig. 7. The phase angle ϕ was held constant for these calculations. A comparison with the peak response magnitude calculated using continuous atomization reveals that order-of-magnitude increases in response magnitude are possible with periodic atomization. Large response magnitudes are calculated for small drops (10 and 25 μm) at all values of atomization frequency. For the larger drop sizes, response magnitude generally increases with decreasing atomization frequency, although peak response values remain above the continuous atomization value. The effects of periodic atomization extend further into the large drop size region as the atomization frequency is decreased.

The effects of periodic atomization on the peak response frequency are considerably less significant, as shown in Fig. 8. Again, the calculated values of peak response frequency

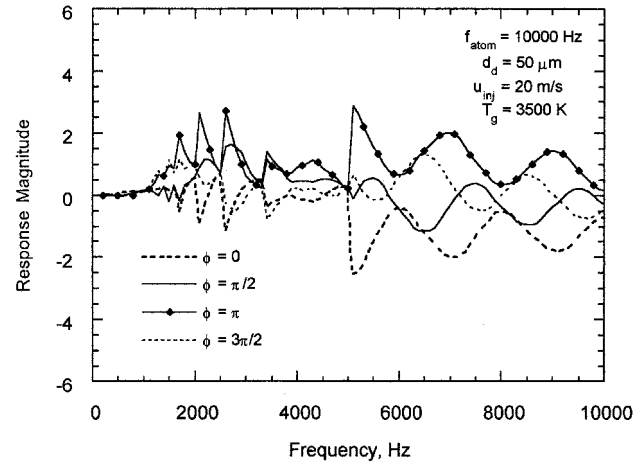

Fig. 6 Vaporization response magnitude as a function of ambient pressure oscillation frequency and phase angle ϕ.

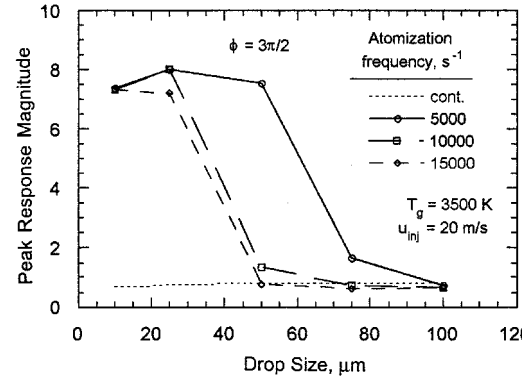

Fig. 7 Peak response magnitude as a function of drop size and atomization frequency for constant phase angle ϕ.

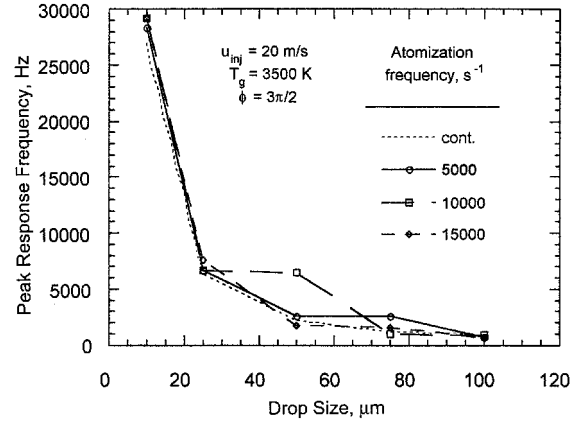

Fig. 8 Frequency at peak response magnitude as a function of drop size and atomization frequency for constant phase angle.

corresponding to continuous atomization are shown for comparison. Generally, the peak response frequency calculated with periodic atomization is consistent with the calculated peak response frequency for continuous atomization, although there were some peculiar cases requiring further study where significant differences occurred.

Experiments

Experiments were conducted to determine the conditions under which periodic atomization could cause longitudinal-mode

combustion instabilities in a model rocket combustor using gaseous oxygen and liquid ethanol as propellants. The gaseous oxygen entered the combustor through a cavity at the injector plane. The experimental setup was composed of the model rocket combustor, an impinging jet injector, piezoelectric drivers, high-frequency pressure transducers, and associated flow delivery and data acquisition equipment. Details of the experimental setup are provided elsewhere.[16]

The chamber used in the combustion modulation tests is 10 in. long, and has a 50.4 × 50.4-mm (2 × 2-in.) internal cross section. The frequency of the fundamental longitudinal mode of the chamber was calculated to be 2200 Hz, based on a 250-mm (10-in.) long combustor and gas properties calculated from a one-dimensional chemical equilibrium program. The combustor was instrumented with high-frequency pressure transducers at approximately 13.0 mm (0.5 in.) downstream of the injection plane and at approximately 38.1 mm (1.5 in.) upstream of the start of the nozzle convergence. This allowed dynamic pressure measurements near the two pressure antinodes. The pressure transducers were calibrated in situ. The linearity of each transducer was 0.363 μV/Pa (2.5 mV/psi). The signal from the high-frequency pressure transducers was sent to a data acquisition system at a rate of 50 kHz, and stored on a personal computer for later analysis. The raw high-frequency pressure signal was also sent to a fast Fourier transform spectrum analyzer for real-time analysis of the power spectral density (PSD) of the chamber pressure oscillations. The PSD was monitored during the tests to evaluate the performance of the electromechanical drivers and to guide the driver configuration.

An impinging jet injector was used, having an orifice diameter of 1.0 mm (0.040 in.) and an included impingement angle of 60 deg. The active injector element was based on technology developed earlier,[17] with the basic design of the electromechanically driven injector assembly shown in Fig. 9. The assembly, 0.152 m (6 in.) in length, is comprised of piezoelectric drivers and a nozzle holder. The driver consists of the piezoelectric transducers, a center bolt, and a piston. Fluid enters the top of the assembly and travels through the hollow center bolt to a fluid manifold, which is formed by the piston surface and an orifice plate. A voltage applied to the transducers causes the piezoelectric material to expand, and the piston is pushed toward the fixed orifice plate. As the voltage to the piezoelectric goes to zero, the center bolt provides the restoring force that draws the piston back to its original position. The voltage signals are provided to the injector system by a function generator, a power amplifier, and matching transformers.[17] The function generator can supply any required signal form, including noise.

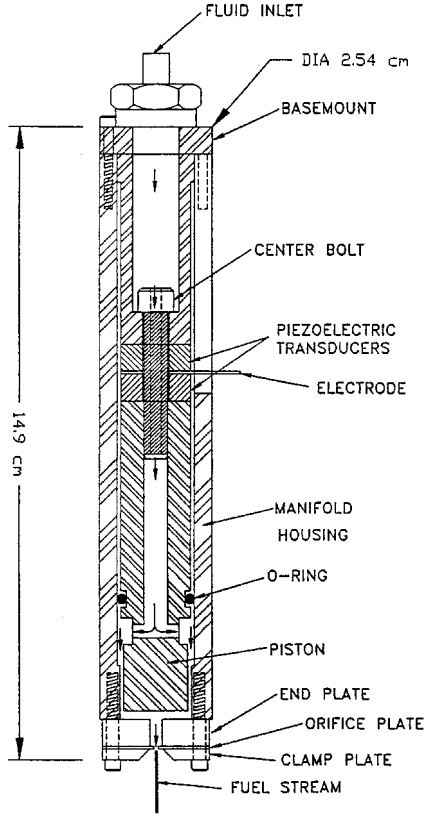

Fig. 9 Electromechanically driven injector assembly.

The electromechanical drivers were incorporated into the injector such that each of the two impinging jets could be driven independently. This allowed different perturbation frequencies to be imposed on the jets, as well as variations in the phase angle between the signal to each jet. Figure 10 is an image of a water spray formed by the driven impinging jet injectors at atmospheric conditions. For the case shown in Fig. 10, the jet velocity is 5.2 m/s, the included impingement angle is 60 deg, and the orifice diameter is 1.0 mm (0.04 in.). The driving force placed on each jet enhances the naturally occurring periodic atomization associated with the impinging jets.

The signals to the electromechanical drivers were established prior to starting the hot-fire test sequence, and left on throughout the test. The drivers were run either at the same frequency, or at different frequencies to produce a beat frequency. Drivers run at the same frequency were run either in-phase or out-of-phase with each other. In-phase driving yielded the highest pressure oscillation amplitude in the combustion tests.

The flexibility of the experimental configuration allowed the test conditions to be changed rapidly. Over 50 variations of driving conditions/flow conditions were tested. The lowest driving frequency tested was 1800 Hz, and the highest driving frequency tested was 8000 Hz. The most effective driving was achieved at the highest flow rate. Chamber pressure and the oxidizer to fuel ratio (O/F) were held relatively constant for all tests, at about 1.45 MPa (210 psia) and 1.7, respectively. The chamber pressure was held constant for different flow rates by changing the nozzle throat diameter.

The frequency of the first longitudinal frequency was calculated to be about 2200 Hz for all conditions. Later it was measured to be about 1850 Hz. The stability parameter in Table 2 is the value of the dimensionless parameter fd_o/U_j, where f is the pressure oscillation frequency (the first longitudinal frequency in this case, 2200 Hz), d_o is the orifice diameter (1 mm), and U_j is the fuel injection velocity (see Table 2). The empirical stability correlation indicated that the stability parameter must be less than about 0.1 for instability to occur. Thus, cases C, D, and E would be capable of driving an instability at the frequency of the first longitudinal mode. Case D also satisfies the condition to drive a second longitudinal mode (f = 4400 Hz, $fd_o/U_j \sim 0.1$). Case E could nearly drive a third longitudinal mode (f = 6600 Hz, $fd_o/U_j \sim 0.12$) as well

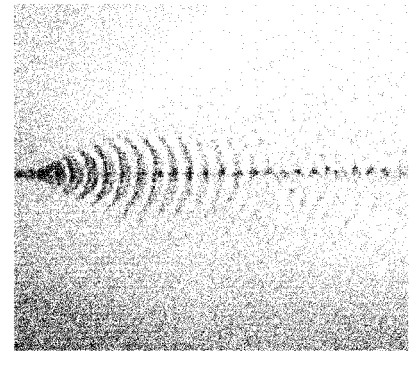

Fig. 10 Spray formed by electromechanically driven impinging injector. Jets are perturbed out-of-phase at 2500 Hz.

Table 2 Combustion modulation test conditions

Operating Parameters	Case A	Case B	Case C	Case D	Case E
$\dot{m}_{fuel}$, kg/s	0.019	0.025	0.031	0.056	0.070
$\dot{m}_{oxidizer}$, kg/s	0.032	0.043	0.053	0.095	0.119
$\dot{m}_{coolant}$, kg/s	0.0068	0.0068	0.0068	0.016	0.016
O/F	1.70	1.71	1.71	1.69	1.69
Pc, MPa	1.43	1.62	1.44	1.57	1.52
D_{throat}, mm	8.76	9.55	11.3	14.6	16.6
f, Hz	2200	2212	2208	2213	2212
U_j, m/s	15	20	25	44	55
fd_o/U_j	0.147	0.110	0.089	0.051	0.0378

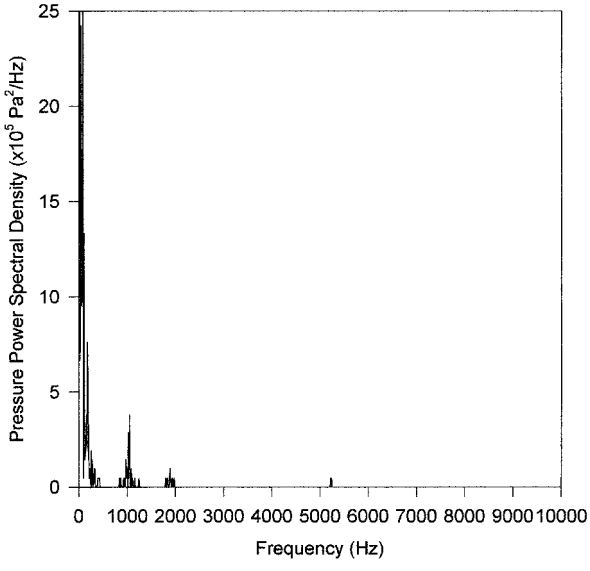

Fig. 11 Pressure PSD. Peaks show first (1850 Hz), second (3700 Hz), and third (5200 Hz) longitudinal modes.

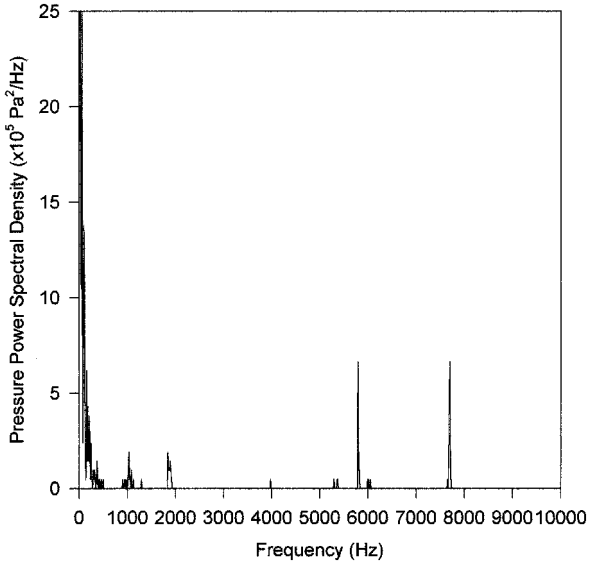

Fig. 12 Pressure PSD. Case E in which jets are driven at 7700 and 5800 Hz to produce a beat frequency of 1900 Hz.

the first and second longitudinal modes, and this was shown to be the case in the experiments.

Results

A plot of the PSD for case E with no signal to the electromechanical drivers is shown in Fig. 11. Significant electronic noise was measured below 600 Hz. Small peaks at about 1850, 3700, and 5200 Hz were measured, corresponding to the first, second, and third longitudinal modes, respectively, and indicating a highly damped chamber. A peak is also observed near 1000 Hz, whose source is not presently known. This peak is observed in all of the results, but is significantly smaller than the larger pressure oscillations observed under conditions for which driving is applied to the jets (see Figs. 12 and 13). It was found that driving the jets near the first longitudinal frequency did not produce significant levels of chamber pressure oscillations. This was primarily because of the low power output of the piezoelectric drivers at frequencies below about 4000 Hz. However, it was possible to drive significant first longitudinal pressure oscillations by causing a beat atomization frequency near 1900 Hz, as shown in Fig. 12. In this case, a 7700-Hz signal was sent to one of the jets, and a 5800-Hz signal was sent to the other jet to produce the beat frequency of 1900 Hz.

The highest levels of pressure oscillations were achieved with high flow rates and driving frequencies of about 5500 Hz, with an in-phase signal provided to the jets as shown in Fig. 13. In this case, both the first and the third longitudinal frequencies were driven. Chamber pressure time traces shown in

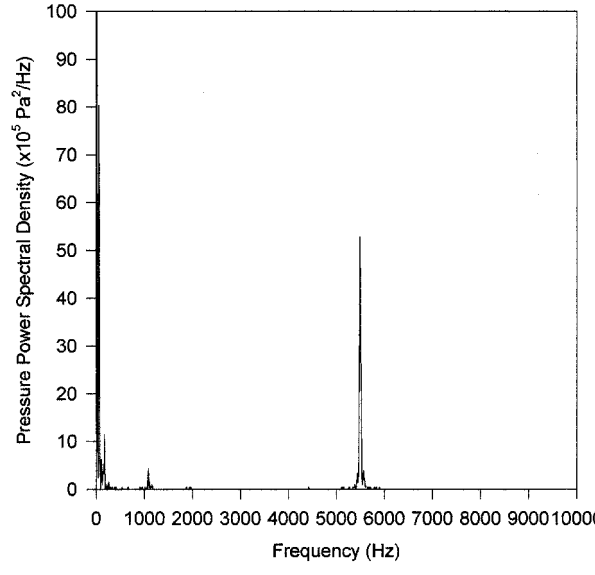

Fig. 13 Pressure PSD. Case E in which jets are driven at 5500 Hz.

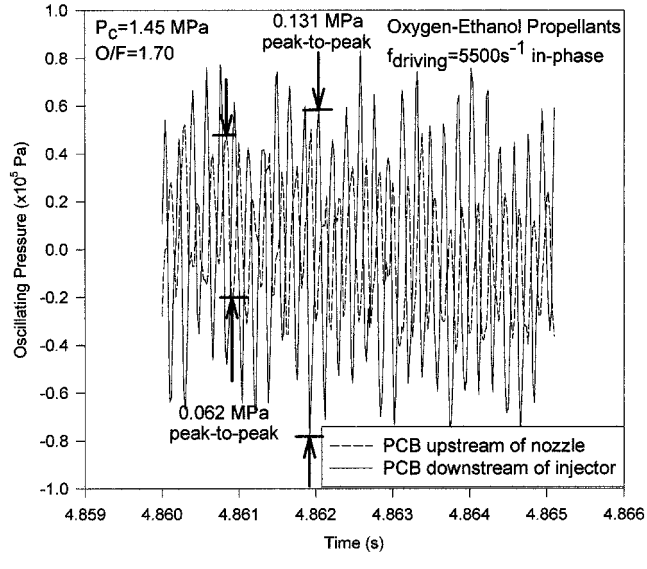

Fig. 14 Time traces of chamber pressure corresponding to the PSD of Fig. 14. The sampling rate is 50 kHz.

Fig. 14 correspond to the plot of PSD shown in Fig. 13 (jets driven at 5500 Hz in-phase). The length of the time slice shown is 5 ms. As shown in Fig. 14, the amplitude of the pressure oscillations for the transducer just downstream of the injector is approximately 0.138 MPa (20 psi) peak-to-peak, or 10% of the chamber pressure. For the case of no driving, the amplitude of the unorganized combustion noise (not shown) is about 13.8 kPa (2 psi) peak-to-peak, or 1% of the chamber pressure.

Summary

To evaluate potential mechanisms of combustion instability, an analysis of the open-loop response of spray combustion to ambient acoustic oscillations was performed. The vaporization of heptane drops in an oxygen environment was considered. Energy release was assumed to occur immediately after vaporization. Experimental results provided a definition of the spray (drop size distribution, mean drop size, atomization frequency) for use as initial conditions.

When atomization occurred continuously, the response analysis results indicated that a wider distribution of drops reduced the response magnitude. A monodisperse size distribution gave the highest response magnitude. However, the response magnitudes for both cases were still lower than the theoretical limit necessary to drive an instability, which is consistent with most previously published results. Calculated peak response frequencies were considerably lower than the highest instability frequency as represented by an empirical stability correlation that has been proven to be accurate for combustors that use impinging jet injectors.

The major effect of including periodic atomization was a large increase in response magnitude. The response magnitude for the cases studied was far above the theoretical limit for driving an instability, and represented as much as an order of magnitude increase over the response magnitude for the continuous atomization case. Generally, the inclusion of periodic atomization did not have a major effect on the peak response frequency.

It was shown that periodic atomization can cause large variations in the response magnitude at acoustic oscillation frequencies as low as 0.1 times the atomization frequency. The increase in response magnitude was largest for small drops. The practice of using arbitrary spacing between drop injection (continuous injection or continuous atomization) yields response magnitudes that are significantly lower than are obtained with realistic atomization frequencies. Although there is evidence that oscillating ambient flowfields can significantly modify the atomization process, the precise mechanism through which coupling occurs is unknown. The analyses presented here indicated that the phase shift associated with the coupling process has an influence on both the peak response frequency and the peak response magnitude. Future work should examine the relationship between ambient pressure oscillations and atomization frequency.

The experimental results provided further evidence that atomization is a key mechanism in driving combustion instabilities. Pressure oscillations at frequencies corresponding to the first through third longitudinal modes were driven in a model combustor using electromechanically driven impinging jets. The ability to drive these very high-frequency pressure oscillations is consistent with the results from an empirical stability correlation. This experimental approach also allows, for the first time, quantitative measurements of the fundamental spray parameters that control the onset of instability.

A theory for a mechanism of combustion instability that is consistent with the results of the analytical and experimental studies presented earlier and the empirical stability correlation can be provided. A reduction in the stability parameter (d_o/U_j), indicating an increased tendency toward instability, implies a reduction in drop size and a reduction in the polydispersity of the spray distribution. According to the analysis presented earlier, however, these effects alone provide only a marginal response magnitude. An additional effect caused by a reduction in the value of the stability parameter is an increase in the atomization frequency. The large variations in response magnitude (which can be well above the theoretical limit for driving an instability), at acoustic oscillation frequencies near the atomization frequency ($f_{osc} \sim 0.1 f_{atom}$) result in a large deposition of energy into a frequency-coupled resonant mode. As the stability parameter decreases, the atomization frequency increases, as does the frequency of the most energized chamber mode. The net result is an increase in the frequency range of combustion instabilities that can be driven, as indicated by the empirical stability correlation.

Acknowledgments

This work was supported by the U.S. Air Force Office of Scientific Research under Grant F49620-97-1-0224, the George C. Marshall Space Flight Center under Contract NAS8-40626, and the Penn State Propulsion Engineering Research Center under Grant NAGW 1356. The authors also acknowledge the help of Ross Hewitt of Aerojet.

References

[1]Anon, "Liquid Rocket Injector Handbook," NASA SP-8089, 1976.

[2]Harrje, D. T., and Reardon, F. H. (eds.), "Liquid Propellant Rocket Instability," NASA SP-194, 1972.

[3]Yang, V., and Anderson, W. E. (eds.), *Liquid Rocket Engine Combustion Instability*, Vol. 169, Progress in Astronautics and Aeronautics, AIAA, Washington, DC, 1995.

[4]Ryan, H. M., Anderson, W. E., Pal, S., and Santoro, R. J., "Atomization Characteristics of Impinging Liquid Jets," *Journal of Propulsion and Power*, Vol. 11, No. 1, 1995, pp. 135–145.

[5]Anderson, W. E., Ryan, H. M., Santoro, R. J., and Hewitt, R. A., "Combustion Instability Mechanisms in Liquid Rocket Engines Using Impinging Jet Injectors," AIAA Paper 95-2357, July 1995.

[6]Anderson, W. E., and Santoro, R. J., "The Effects of Drop Size Distribution and Atomization Periodicity on Combustion Response," AIAA Paper 96-3027, July 1996.

[7]Heidmann, M. F., and Wieber, P. R., "An Analysis of the Frequency Response Characteristics of Propellant Vaporization," NASA TN D-3749, 1966.

[8]Priem, R. J., and Heidmann, M. F., "Propellant Vaporization as a Design Criterion for Rocket Engine Combustion Chambers," NASA TR R-67, 1960.

[9]Tong, A.-Y., and Sirignano, W. A., "Oscillatory Vaporization of Fuel Droplets in an Unstable Combustor," *Journal of Propulsion and Power*, Vol. 5, No. 3, 1989, pp. 257–261.

[10]Anderson, W. E., Ryan, H. M., and Santoro, R. J., "A Model for Impinging Jet Injector Atomization," *32nd JANNAF Combustion Subcommittee Meeting and Propulsion Engineering Research Center 7th Annual Symposium*, Vol. II, CPIA Publication 631, Columbia, MD, 1995, pp. 55–64.

[11]Hasson, D., and Peck, R. E., "Thickness Distribution in a Sheet Formed by Impinging Jets," *AIChE Journal*, Vol. 10, No. 5, 1964, pp. 752–754.

[12]Dombrowski, N., and Hooper, P. C., "The Performance Characteristics of an Impinging Jet Atomizer in Atmospheres of High Ambient Density," *Fuel*, 1962, pp. 323–334.

[13]Priem, R. J., and Guentert, D. C., "Combustion Instability Limits Determined by a Nonlinear Theory and a One-Dimensional Model," NASA TN D-1409, 1962.

[14]Muss, J. A., Nguyen, T.-V., and Johnson, C. W., "User's Manual for Rocket Combustor Interactive Design (ROCCID) and Analysis Computer Program," NASA CR 187110, 1991.

[15]Strahle, W. C., and Crocco, L., *Analytical Investigation of Several Mechanisms of Combustion Instability, Bulletin of the 5th Liquid Propulsion Symposium*, Vol. 2, CPIA Publication 34, Columbia, MD, 1963.

[16]Anderson, W. E., "Demonstration of Combustion Modulation Techniques for Active Control of High-Energy-Density Propellant Combustion in Rocket Engines," NASA Marshall Space Flight Center, Final Rept., Contract NAS8-40626, Huntsville, AL, Dec. 1996.

[17]Dressler, J. L., "Two-Dimensional, High-Flow, Precisely Controlled Monodisperse Drop Source," Aero Propulsion and Power Directorate, Wright Laboratory, U.S. Air Force Material Command, Final Rept., WL/TR-93-2049, Wright–Patterson AFB, OH, March 1993.